Evaluation of Chemical Structures and Work Function of NiSi near the Interface between NiSi and SiO_2

Hideki MURAKAMI[1], Akio OHTA[1], Hiromichi YOSHINAGA[1], Daisuke AZUMA[1],
Yuuki MUNETAKA[1], Seiichiro HIGASHI[1], Seiichi MIYAZAKI[1],
Takayuki AOYAMA[2], Kimihiko HOSAKA[2], Kentaro SHIBAHARA[1,3]

[1]Grad. School of AdSM, Hiroshima Univ., Kagamiyama 1-3-1, Higashi-Hiroshima 739-8530, Japan
[2]Fujitsu Laboratories Ltd., [3]Research Center for Nanodevices and Systems, Hiroshima Univ.
E-mail: semicon@hiroshima-u.ac.jp

1. Introduction

Continuous scaling of complementary metal-oxide-semiconductor field effect transistors (CMOSFETs) inevitably requires an increase in capacitive coupling between the gate and the channel while maintaining an allowable leakage current level through a gate dielectric.

In this regard, many efforts have been made to replace conventional silicon oxynitride with physically thicker but electrically thinner High-k gate dielectrics [1-3]. Meanwhile, the use of conventional poly-Si gate is faced practically with serious limitations related to gate potential drop caused by the gate leakage current flowing through a gate resistance [4], a depletion effect [5,6] and a Fermi level pinning [7,8] phenomenon emerging in combination with high-k gate dielectrics.

To overcome such limitations, the implementation of alternative gate materials with lower resistivity is needed. Silicides such as NiSi are thought to be promising candidates for metal gates [9-11].

The control of the work function of silicides is one of the major isssues for the implement of Silicide gate. Although the work function of silicides can be controlled to some extent by a change in chemical composition and/or impurity doping, even in the case of NiSi in which the Fermi level is located inherently around the Si midgap(4.6eV~4.7eV), it is difficult to obtain the values suitable for n- and p-MOSFETs [11].

In this work, pure and impurity-implanted Ni-silicides formed on SiO_2 were characterized by X-ray photoelectron spectroscopy (XPS), where the Ni-silicide/SiO_2 interfaces were analyzed through SiO_2 for the samples after removing the Si substrate from the backside in addition to the analysis from the surface side to evaluate the correlation between the effective work function and chemical composition or impurity concentration at the interface.

2.Experimental

After standard wet-cleaning steps of the Si(100) wafers, a 7.0nm-thick SiO_2 was grown on the surface by thermal oxidation and 100nm thick poly-Si was grown by LPCVD. Subsequently, a part of samples, Impurity (Sb, P, B and As) was implanted with a dose of $1.0x10^{16}cm^{-3}$, 2-step silicidation annealing was performed at the temperature of 400 and 500°C

.

For measuring the interface between NiSi/SiO_2, Si substrate was removed completely by wet chemical etching of $HF:HNO_3:CH_3COOH:C_2H_5OH$ compound solution down to the thickness of about 10μm.

For the thinkness range thinner than 10μm, the Si selective etching was performed by KOH solution with thickness monitoring. After the SiO_2 layer exposuring, the chemical bonding features and work function were evaluated by XPS and Raman scattering spectroscopy.

3. Results and discussion

Figure 1 shows a Raman spectrum for undoped NiSi measured from Si substrate side were performed at each steps of back-side etching. As etching progressed, Si TO phonon peak intensity($520cm^{-1}$) from Si substrate is decreased, and the signals from NiSi phase become remarked. After removing Si substrate completely, the optical phonon signal from NiSi phase is dominant and signals from $NiSi_2$ is observable slightly, which suggest

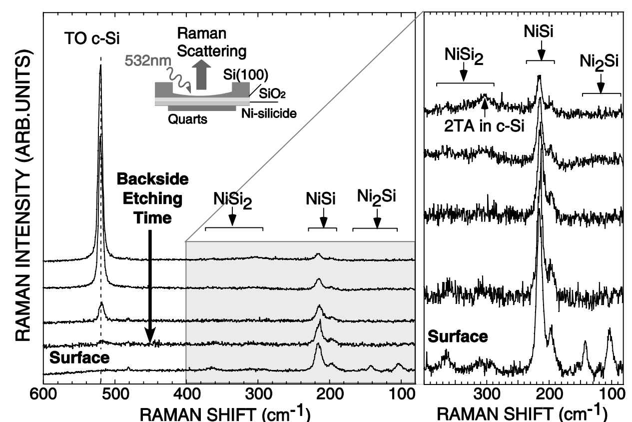

Fig. 1 Change in Raman spectra for undoped Ni-Silicide during back side etching process.

that the component of NiSi around Ni-silicide/SiO_2 interface is Si rich. The chemical bonding features and chemical composition at the Ni-silicide/SiO_2 interface after back-side etching and Ni-silicide surface was measured by using hard X-ray(8kev) and soft X-ray(1.486keV) photoelectron spectroscopy. Hard X-ray photoelectron spectroscopy(HXPES) give us deeper proving depth than that of soft X-ray.

Figure 2 shows P1s spectra for the P doped sample at the sureface and the interface measured by HXPES. The peak intensity is normalized with peak intensity of Ni-silicide component on Ni2p3/2. The signals due to Ni-P or Si-P bonding unit is dominated and oxided P componet is slightly observed. The peak intensity of P1s signal measured from the surface with lowering take-off angle, which implies that P atom is piled up at Ni-Silicide surface. In addition, The peak intensity measured from back side through SiO_2 layer is a few times larger than that measured from surface side, resulting that P atoms piled up at the interface. Similar result as P implanted sample can be obtained for the As implanted sample.

High resolution XPS with monocromatic AlKa X-ray, the chemical bonding features near Ni-silicide/SiO_2 interface measured from back side(Fig. 3). From Ni2p3/2 spectra, the signals due to Ni-silicide is dominant for the case measured from both surface and interface, and oxided Ni component(NiO: ~854eV, Ni_2O_3:~856eV) were hardly observed. Chemical bonding features at the Ni-silicide/SiO_2 interface were compared with those at the Ni-silicide surface as shown in Fig.4. For the pure Ni-silicide sample prepared without implantation, Ni2p 3/2 signals originated from Ni-Si bonding units were clearly observed at a binding energy of ~853eV and almost no oxide component of Ni was observable both at the Ni-silicide surface and at the Ni-silicide/SiO_2 interface. The formation of Si-O bonds at the surface and at the interface was confirmed from Si2p spectra. Chemically-shifted Si2p signals the due to Si-O bonding units were broadened toward the lower binding energy side even for the Si2p spectrum measured through the SiO_2 layer after the back side etching, in comparison to the reference spectrum of 2nm-thick thermally-grown SiO_2 on Si(100). This result indicates that the interface between Ni-Silicide and SiO_2 is not atomically flat. Notice that the average chemical composition Ni/(Ni+Si) at the interface was Si-rich as compared with that at the Ni-silicide surface.

Similar results are obtained for implanted samples except the B-implanted case where both at the surface and at the interface were Si-rich. The chemical bonding features of implanted impurities such as Sb, B and P near the Ni-silicide/SiO_2 interface were investigated in comparison to those near the Ni-silicide surface as shown in Fig.4. For

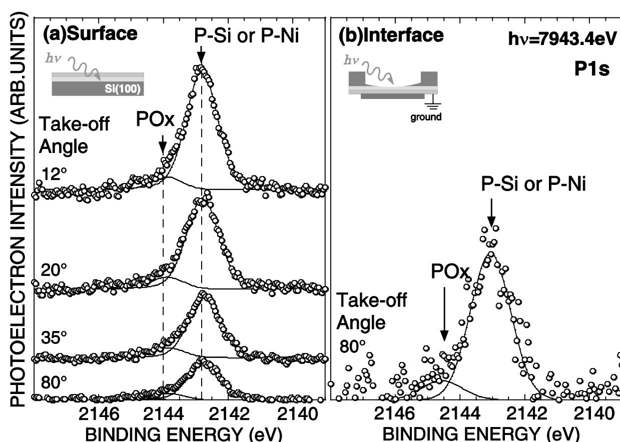

Fig. 2 P1s spectra of P doped sample at the surface(a) and Ni-Silicide/SiO2 interface(b).

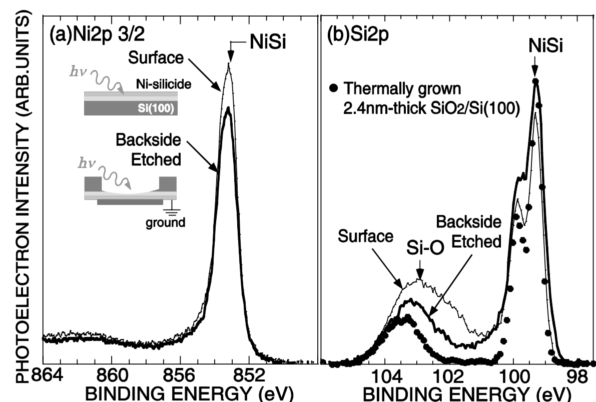

Fig. 3 Ni2p3/2(a) and (b)Si2p(b) spectra of undoped sample at the Ni-Silicide/SiO2 interface.

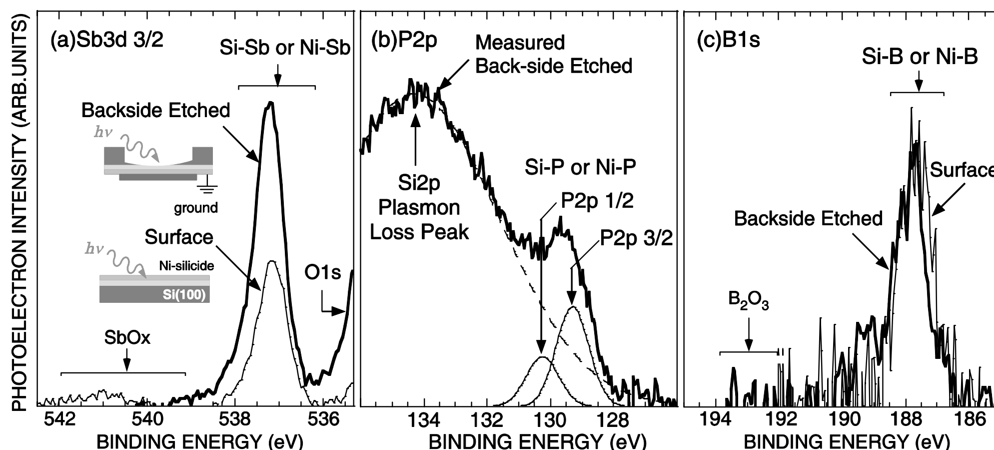

Fig. 4 Sb3d3/2, P2p and B1s spectra of impurity doped sample at the surface and Ni-Silicide/SiO2 interface.

Table *1* Average chemical compositions of Ni-silicide at the surface and Ni-silicide/SiO2 interface.

Sample		Chemical Composition (at.%)						Ni/(Ni+Si) (%)
		Si	Ni	Sb	B	P	As	
non	surface	51.8	48.2	–	–	–	–	48.2
	interface	63.0	37.0	–	–	–	–	37.0
Sb	surface	48.8	49.8	1.4	–	–	–	50.5
	interface	71.1	18.0	10.9	–	–	–	20.2
B	surface	67.5	24.1	–	8.4	–	–	26.3
	interface	71.2	22.8	–	6.0	–	–	24.3
P	surface	44.3	55.7	–	–	0.0	–	55.7
	interface	90.3	7.8	–	–	1.9	–	7.8
As	surface	43.0	57.0	–	–	–	0.0	57.0

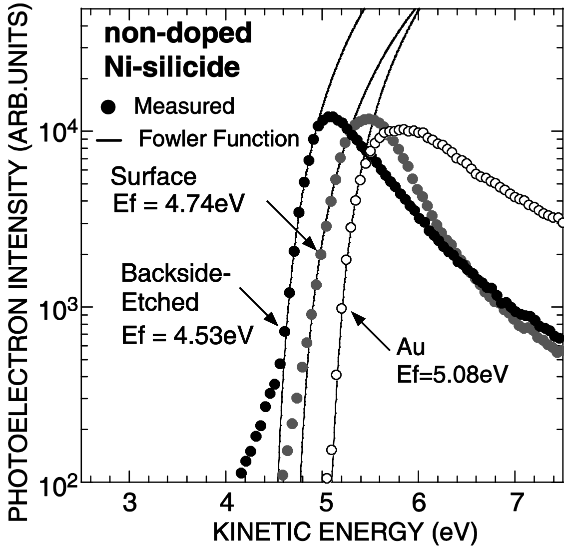

Fig.5. The yield spectra near the Fermi edge for the surface and at the interface of the pure Ni-silicide sample. The yield spectra for the Au after removing surface carbon contaminants by Ar+ ion sputtering were also shown as references. In addition, the curve fittings to the measured spectra with the use of a Fowler function are demonstrated.

all cases, impurities bonded with Ni and/or Si atoms are dominant. No incorporation of implanted Sb and P into the thermally-grown SiO_2 layer and native surface oxide was observable but in contrast distinct pile-ups of Sb and P atoms near the Ni-silicide/SiO_2 interface were detected. On the other hand, for the B-implanted case, chemically-shifted B1s signals presumably due to suboxides were slightly observed at the Ni-silicide/SiO_2 interface and no pile-up of B atoms at the interface was measured.

Photo-excited electrons passing though materials can suffer inelastic scatterings and lose their energy with some electronic excitations. If the kinetic energy of excited electrons becomes or is below the work function of a metallic material of interest, such a low energy electron can no longer emit to the outside. Thus, the work function of can be determined from the threshold energy for photoelectrons near the lower limit in the kinetic energy scale. With consideration of the Fermi distribution at room temperature, based on the Fowler theory, we determined the work function from the energy shift fitted by which a Fowler function at room

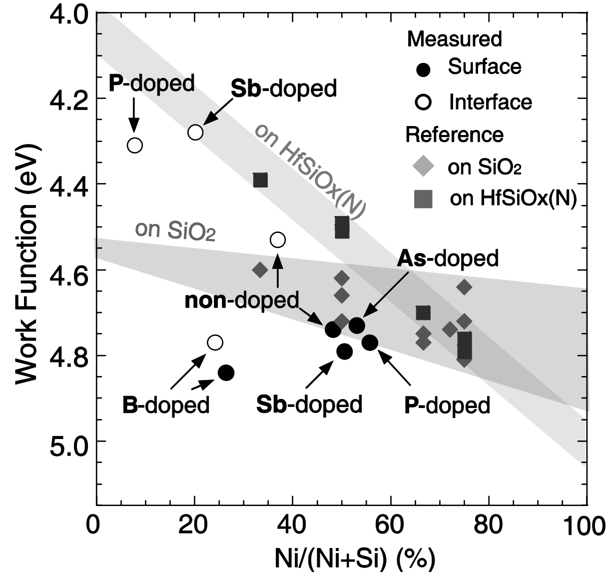

Fig.6. Effective work functions of the surfaces and the interfaces of Ni-silicides prepared with and without impurity implantation, which were determined by XPS measurements.

temperature to the measured photoelectron spectrum near the lower limit in the kinetic energy scale [15].

In this work, to detect sufficient photoelectrons emitting with a low kinetic energy, negative bias as low as -15V was applied to the sample. For the calibration of this technique and setting a proper sample bias, we first measured the work functions of pure metals such as Au, Ni and Pt and confirmed that the measured values are the same as the reported ones within an accuracy of ±0.05eV.

As represented in Fig. 5, by fitting a Fowler function to the measured spectra for undoped sample, the work function at the surface and the interface were 4.74eV and 4.53eV, respectively. The chemical composition at the interface is silicon rich as discussed already, so the work function lowering at the interface can be interpreted in terms of the chemical composition.

The effective work functions for doped samples as a function of Ni composition (Ni/(Ni+Si) (%)) were summarized in Fig. 6, and the reported work function of Ni-silicide formed on SiO_2 or $HfSiO_x$(N[6-9]) is represented as a refer. The work fuctions at the surface is almost ~4.8eV, no significant difference can be observed. The effective work function at Ni-silicide /SiO_2 interface tend to be lowered in comparison with that at the surface as can be seen in the case of undoped sample. Notice that, for the Sb doped sample, the work function at the interface is lowered by ~0.5eV than that at surface, which is thought to be originated in the Ni composition change and Sb atom pile-up up to 11% at the interface. The work function of Sb doped samples on Ni compsition is similar to the reported work function change of Ni-silicide on $HfSiO_x$(N). The work function lowering of P doped sample at the interface side represent similar trend as Sb implanted sample. However, the pile-uped P atom is

only 1.9at.%, so the effective workfunction lowering affects presumably the decrease in Ni composition.

4. Conclusions

The chemical bonding feautures and effective work function of impurity doped(B, P, As and Sb) Ni-silicide /SiO_2 interface were evaluated by Raman scattering spectroscopy and XPS analysis through SiO_2 by Si substrate removing. At the surface, Ni_2Si, NiSi and $NiSi_2$ phase are mixed. However, at Ni-silicide/SiO_2 interface NiSi phase is dominant. It is highly possible that the control of chemical composition is more useful for the control of work function rather than the control of impurity pile-up. Meanwhile, for B-implanted Ni-silicide, B incorporation suppress a reduction in the work function with a decrease in Ni composition.

Acknowledgments

This work was partly supported by STARC. The synchrotron radiation experiments were performed at SPring-8 with the approval of Japan Synchrotron Radiation Research Institute (JASRI) as Nanotechnology Support Project of the Ministry of Education, Culture, Sports, Science and Technology. (Proposal No. 2005B0410-Nsa-np-Na / BL-No.47XU)

References

[1] M.Fukuda, W. Mizubayashi, A. Kohno, S. Miyazaki and M. Hirose, Jpn. J. Appl. Phys. 37, L1534 (1998).

[2] G.D. Wilk, R.M. Wallace and J.M. Anthony, J. Appl. Phys. 89, p.5243 (2001).

[3] M.L. Green, E.P. Gusev, R. Degraeve and E.L. Garfunkel, J. Appl. Phys. 90, 2057 (2001).

[4] M. Koh, W. Mizubayashi, K. Iwamoto, H. Murakami, T. Ono, M. Tsuno, T. Mihara, K. Shibahara, S. Miyazaki and M. Hirose, IEEE Trans. Elect. Dev. 48, 259 (2001).

[5] R. Rios, N.D. Arora, and C.-L. Huang, IEEE Electron Device Lett. 15, 129 (1994).

[6] N.D. Arora, R. Rios and C.-L. Huang, IEEE Trans. Elect. Dev. 42, 935 (1995).

[7] C. Hobbs, L. Fonseca, A. Knizhnik, V. Dhandapani, S. Samavadam, B. Taylor, J. Grant, L. Dip, D. Triyoso, R. Hegde, D. Gilmer, R. Garcia, D. Roan, L. Lovejoy, R. Rai, L. Hebert, H. Tseng, S. Anderson, B. White and P. Tobin, IEEE Trans. Elect. Dev. 51, 978 (2004).

[8] K. Shiraishi, K. Yamada, K. Torii, Y. Akasaka, K. Nakajima, M. Konno, T. Chikyow, H. Kitajima and T. Arikado, Jpn. J. Appl. Phys. 43, L1413 (2004).

[9] J. Kedzierski, E. Nowak, T. Kanarsky, Y. Zhang, D. Boyd, R. Carruthers, C. Cabral and R. Amos, Tech. Dig. IEEE Int. Electron Device Meeting, p.247 (San Francisco, 2002).

[10] J. Kedzierski, D. Boyd, P.Ronsheim, S. Zafar, J. Newbury, J. Ott, C. Cabral Jr., M. Ieong and W. Haensch, Tech. Dig. IEEE Int. Electron Devices Meeting, p. 315 (Washington, 2003).

[11] C. Cabral, Jr., J. Kedzierski, B. Linder, S. Zafer, V. Narayanan, S. Fang, A. Steegen, P. Kozlowski, R. Carruthers and R. Jammy, VLSI Symp. Tech. Dig. p.184 (2004).

[12] F.U. Hillebrechit, J.C. Fuggle, P.A. Bennett and Z. Zolnierek, Phys. Rev. B 27, 2179 (1983).

.